Hindawi
Mathematical Problems in Engineering
Volume 2020, Article ID 7469470, 14 pages
https://doi.org/10.1155/2020/7469470

Research Article

Dynamic Safety Management on the Key Equipment of Coal Gasification Based on Dbt-Dbn Method

Han Gao,[1] Yili Duo ,[1,2] Tie Sun,[1] and Xuefeng Yang[1]

[1]*School of Mechanical Engineering, Liaoning Shihua University, Fushun 113001, China*
[2]*College of Pipeline and Civil Engineering, China University of Petroleum, Qingdao 266580, China*

Correspondence should be addressed to Yili Duo; lnpuduoyili@163.com

Received 6 July 2020; Accepted 18 September 2020; Published 7 October 2020

Academic Editor: Francisco J. Montáns

Gasifier system is one of the important components of coal gasification device. The technical characteristics of this system mainly lie in the following facts as huge technical scale and high complexity, and there is a dynamic correlation between the failure modes of gasification equipment. Traditional safety analysis methods such as fault tree and bow-tie diagram suffer from drawbacks as being static and ineffective in handling uncertainty, which hamper their application to risk analysis of process systems. This paper presents a newly developed model based on Dynamic Bow-Tie (DBT) and Dynamic Bayesian network (DBN) for quantitative dynamic risk assessment of gasifier system. In the meantime, in order to cope with the uncertainty of the failure data, fuzzy numbers and the defuzzification method are used to transform the experts' language into the failure rates. The results showed that dynamic risk assessment can solve the difficulties dealing with complex dynamic systems which have process variables and characteristics such as multiple, failure correlations, and noncoherence. And it also has important theoretical significance and application value for coal chemical industry to improve the scientificity of risk assessment.

1. Introduction

Coal gasification plays an important role in human history, and this technology has been widely developed throughout the world, especially after the oil crisis in the 1970s [1–3]. China is a typical "rich coal, lean oil, and low gas" country; coal energy accounts for more than 65% from the perspective of energy structure [4–6]. Coal gasification is a new industry; China's shortage of oil and gas resources can be remedied by developing a safe, green, and environmentally coal gasification. With widespread and successful applications, this technology has greatly promoted the development of the coal chemical industry in China [1]. The water-coal slurry gasification process is under simultaneous conditions of high temperature and high pressure; water-coal slurry and oxygen undergo a fierce redox reaction in the gasifier and generate syngas. The syngas is an inflammable and explosive mixed gas, so once an accident happens, it will not only lead to property loss, but also cause casualties and even environmental pollution. Therefore, as the key equipment of water-coal slurry gasification, it is necessary to analyze and describe the risk factors of the gasifier in this paper.

There also have been some researches regarding security problem in coal gasification process [7–10]. Reference [11] reported many accidents in gasification plants during the last 20 years in the world; the researchers suggest that more careful concentration is needed during the design of the coal gasifier and the preparation of the constructed gasifier operation. Reference [12] developed a comprehensive technique to control the major hazards of the GE coal gasification process. The technique consisted of process hazard identification based on critical events, barrier performance evaluation based on barrier diagrams, and quantification of risk influence factors based on Bayesian network. Reference [13] introduced an efficient methodology utilizing improved Signed Directed Graph for the HAZOP analysis, and an industrial case about the coal conveying in a complex process of coal gasifier is modeled and analyzed. Although these

researches focused on the safety issues in coal gasification process, the risk assessment methods applied in these researches were not dynamic, it encountered many difficulties in dealing with the safety assessment of complex systems such as polymorphism, nonmonotonicity, failure correlation [14], dynamics [15], process variables, and other influencing factors [12].

Dynamic risk assessment approaches can significantly reduce both the potential for hazardous events and undesirable consequences [16]. In turn, it increases the safety of the operation and reliability of the systems; it is an extension of the definition of risk taking into account the time-varying characteristics. With respect to the dynamic risk assessment approaches, many researchers have done much work on it. Reference [17] proposed a complete set of dynamic risk assessment to predict the frequencies of abnormal events utilizing accident precursor data, helping to achieve inherently safer operations. Based on these methods, the failure probabilities of safety systems and end-states were estimated using copulas and Bayesian analysis to ensure better predictions. The method was further developed by Kalantarnia et al. [18], where a model was established. The model has used Bayesian theory to revise the risk profile, denoted as the posterior risk function, based on real-time data from the system. As pointed out in [19], Bayesian networks (BNs) have become a popular tool for quantitative risk assessment. Reference [20] aimed at developing dynamic safety analysis methodology for the offloading process for FLNG platforms using BN analysis. The purpose of conducting this safety assessment is to advance better understanding of the floating liquefied natural gas (FLNG) concept during the construction phase [20]. Zarei et al. [21] applied BN to model accident scenarios of natural gas stations for risk assessment. However, BN is time-independent, and it cannot reflect temporal evolution of system and give prevention measures effectively. To this end, dynamic Bayesian network (DBN) [22–24] has been introduced, and it is equipped with other techniques such as bow-tie model [25, 26]. This composite model has been applied to quantitative risk analysis of hydrogen generation unit leakage [27] and offshore drilling incidents [28]. Nevertheless, a composite analysis model of coal-water slurry gasifier accidents is not available; few studies concern this issue.

The present paper attempts to integrate DBN and dynamic bow-tie model [29] for dynamic risk analysis of coal-water slurry gasifier failure. Meanwhile, fuzzy numbers and the defuzzification method are used to transform the experts' language into the failure rates, solving the problem that it is difficult to obtain a large amount of historical statistical data. The rest of the paper is organized as follows: A brief description of theoretical basis for dynamic bow-tie model and dynamic Bayesian networks is presented in section 2. Conversion rules and processing of DBN model are specifically described in section 3. The proposed method is applied for dynamic risk analysis of gasifier heating in the case study of section 4. Finally, the conclusions of this study are presented in section 5.

2. Theoretical Basis for Dynamic Bow-Tie Model and DBN

2.1. Dynamic Bow-Tie Model. The bow tie model is an accident causality analysis method that combines fault tree and event tree analysis methods into one; this method can not only comprehensively analyze the causes and consequences of an event, but also clearly and intuitively describe the timing of the accident and the logical relationship of each event. The bow tie model is characterized by a fault tree on its left-hand side and event tree on its right-hand side with a "bottom event" in its center.

Dynamic bow tie model adds sequential notion to traditional FT method, building a complex system failure model, as shown in Figure 1 As an extension of ordinary static bow-tie, the dynamic bow-tie analysis not only includes Boolean logic relation but also includes dynamic logic gates (e.g., PAND, SEQ, SPARE, and FDEP), and some events' reliability changes over time.

2.2. DBN. A static Bayesian network (BN) as a probability-based knowledge representation method is appropriate for the modeling of causal processes with uncertainty; it models a system at a fixed time [30, 31]. A DBN extends the notion of a Bayesian network to model the stochastic evolution of a set of random variables over time. To quantify the timing of discrete changes in the data, the state distribution at each moment contains a Bayesian network called a time slice. Therefore, structure and parameters in DBN do not vary over time, which reflects only the time-varying process of sample data. Then DBN can be split into an initial network and a transition network, representing the initial network as a probability distribution at the initial moment, transition network is expressed as transition probability distribution of adjacent time slices, as shown in equation (1):

$$P\left(X_t \mid X_{t-1}\right) = \prod_{i=1}^{N} P\left(X_i^t \mid \mathrm{Pa}\left(X_i^t\right)\right). \tag{1}$$

Figure 2 is a structural diagram of DBN; different colors are used to distinguish nodes and directed arcs of different time slices. DBN's conditional probability can be divided into intra-slice CPT and inter-slice CPT. If a DBN can expend T time slices, the joint probability distribution of these T time slices is

$$P\left(X_{1:T}\right) = \prod_{t=1}^{T} \prod_{i=1}^{N} \left(PX_t^i \mid \mathrm{Pa}\left(X_t^i\right)\right). \tag{2}$$

3. Conversion Rules and Processing of DBN Model

DBN can be constructed directly from an understanding of sequential systems, while considering the existence of a large number of static/dynamic fault trees. DBN is modeled based on the existing FT model. Because historical information can be used for reference, this method not only effectively avoids subjectivity but also improves reliability. Meanwhile, this

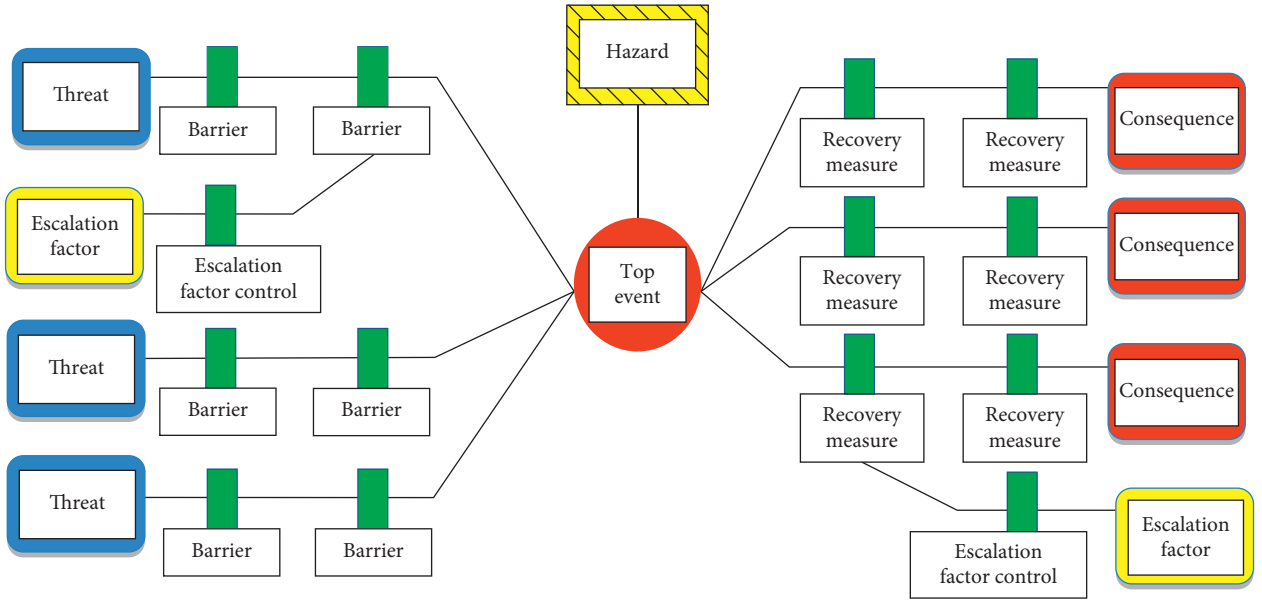

Figure 1: Dynamic bow-tie model.

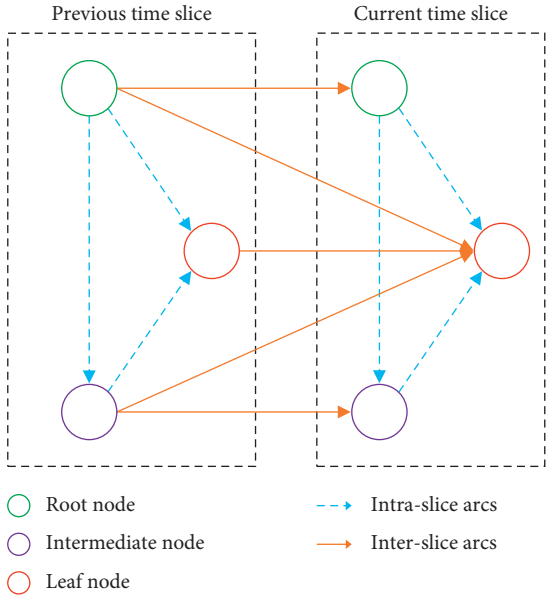

Figure 2: Dynamic Bayesian network diagram.

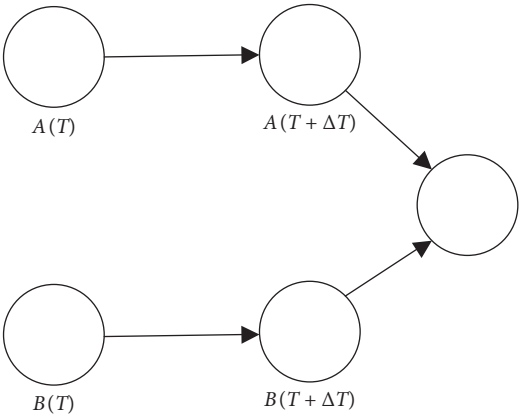

Figure 3: "AND gate," "Or gate" logical relationship.

method also implements the method of automatic network construction by utilizing the rules of static/dynamic fault tree conversion to DBN, reducing the difficulty of DBN modeling.

3.1. Transformation of Static Logic Gates. Assume $E=0$ means that event E does not occur, $E=1$ means that event E occurs, $f_E(t)$ is the probability density function of the time when E occurs.

3.1.1. And Gate. Figure 3 shows the DBN corresponding to the logical relationship of "AND gate", and the node conditional probability distribution is as follows:

$$P\{A(T+\Delta T)=1 \mid A(T)=0\} = \int_{T}^{T+\Delta T} f_A(t)\mathrm{d}t, \tag{3}$$

$$P\{A(T+\Delta T)=1 \mid A(T)=1\} = 1, \tag{4}$$

$$P\{B(T+\Delta T)=1 \mid B(T)=0\} = \int_{T}^{T+\Delta T} f_B(t)\mathrm{d}t, \tag{5}$$

$$P\{B(T+\Delta T)=1 \mid A(T)=1\} = 1, \tag{6}$$

$$P\{\mathrm{TE}=1 \mid A(T+\Delta T)=1, B(T+\Delta T)=1\} = 1, \tag{7}$$

$$P\{\mathrm{TE}=1 \mid \mathrm{else}\} = 0. \tag{8}$$

3.1.2. Or Gate. The DBN corresponding to the "Or gate" logic is consistent with Figure 3 the conditional probability

distribution of $A(T+\Delta T)$ and $B(T+\Delta T)$ is the same as in equations (1)–(4). The conditional probability distribution of the node TE is shown as follows:

$$\begin{aligned} P\{\mathrm{TE}=1 \mid A(T+\Delta T)=1\}&=1,\\ P\{\mathrm{TE}=1 \mid B(T+\Delta T)=1\}&=1,\\ P\{\mathrm{TE}=1 \mid A(T+\Delta T)=0, B(T+\Delta T)=0\}&=0. \end{aligned} \tag{9}$$

3.1.3. Not Gate. Figure 4 shows the DBN corresponding to the "not gate" logical relationship. The conditional probability distribution of $A(T+\Delta T)$ is the same as in equations (1) and (2). The conditional probability distribution of the node TE is shown as follows:

$$\begin{aligned} P\{\mathrm{TE}=1 \mid A(T+\Delta T)=1\}&=0,\\ P\{TE=1 \mid A(T+\Delta T)=0\}&=1. \end{aligned} \tag{10}$$

3.2. Dynamic Logic Gate Transformation

3.2.1. Priority And Gate. Priority And gate includes several input events, and output events occur when they happen in a specific order, as shown in Figure 5. If events A, B, and C all occur, and event A occurs before event B, and event B occurs before event C, the output event will occur. Conversely, if not all three input events occur, or event B occurs before event A or event C occurs before event B, the output event will not occur. It is important to point out that if the input events occur at the same time, it is considered that the output event also occurs.

According to sequential and logical relationship of the priority and gate, two binary state nodes FS1 and FS2 need to be added. Among them, FS1 = 1 means that A happened before B, FS2 = 1 means B happened before C, FS1 = 0 means A did not happen before B, FS2 = 0 means B did not happen before C. The relationship between the Priority And gate and the DBN is shown in Figure 5, the conditional probability distribution of each node is

$$\begin{cases} P\{A(T+\Delta T)=1 \mid A(T)=0\}=\int_T^{T+\Delta T} f_A(t)\mathrm{d}t,\\ P\{A(T+\Delta T)=1 \mid A(T)=1\}=1,\\ P\{B(T+\Delta T)=1 \mid B(T)=0\}=\int_T^{T+\Delta T} f_B(t)\mathrm{d}t,\\ P\{B(T+\Delta T)=1 \mid A(T)=1\}=1,\\ P\{C(T+\Delta T)=1 \mid C(T)=0\}=\int_T^{T+\Delta T} f_C(t)\mathrm{d}t,\\ P\{C(T+\Delta T)=1 \mid C(T)=1\}=1,\\ P\{\mathrm{FS1}(T+\Delta T)=1 \mid \mathrm{FS1}(T)=1\}=1,\\ P\{\mathrm{FS1}(T+\Delta T)=1 \mid A(T)=1, \mathrm{FS1}(T)=0\}=1,\\ P\{\mathrm{FS1}(T+\Delta T)=1 \mid A(T)=0, \mathrm{FS1}(T)=0\}=0,\\ P\{\mathrm{FS2}(T+\Delta T)=1 \mid FS2(T)=1\}=1,\\ P\{\mathrm{FS2}(T+\Delta T)=1 \mid B(T)=1, FS1(T)=0\}=1,\\ P\{\mathrm{FS2}(T+\Delta T)=1 \mid B(T)=0, FS1(T)=0\}=0,\\ P\{\mathrm{PAND}=1 \mid A(T+\Delta T)=B(T+\Delta T)=\mathrm{FS1}(T+\Delta T)\\ =\mathrm{FS2}(T+\Delta T)=1\}=1. \end{cases} \tag{11}$$

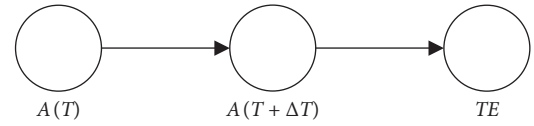

Figure 4: "Not gate" logical relationship.

3.2.2. Sequence-Correlated Gate. The sequence-correlated gate includes several input events, which require the input events to occur in a specific order (from left to right). Unlike priority and gates, sequence-correlated gates force their input events to occur only in a specific order. According to the temporal logic relationship of sequence-correlated gates, analyze the function-correlated gates of the three basic events in Figure 6 to obtain the dynamic Bayesian network corresponding to them, and the conditional probability distribution of each node is

$$\begin{cases} P\{A(T+\Delta T)=1 \mid A(T)=1\}=1,\\ P\{A(T+\Delta T)=1 \mid A(T)=0\}=\int_T^{T+\Delta T} f_A(t)\mathrm{d}t,\\ P\{B(T+\Delta T)=1 \mid A(T)=0, B(T)=0\}=0,\\ P\{B(T+\Delta T)=1 \mid A(T)=1, B(T)=0\}=\int_T^{T+\Delta T} f_B(t)\mathrm{d}t,\\ P\{B(T+\Delta T)=1 \mid B(T)=1\}=1,\\ P\{C(T+\Delta T)=1 \mid B(T)=0, C(T)=0\}=0,\\ P\{C(T+\Delta T)=1 \mid B(T)=1, C(T)=0\}=\int_T^{T+\Delta T} f_C(t)\mathrm{d}t,\\ P\{C(T+\Delta T)=1 \mid C(T)=1\}=1,\\ P\{\mathrm{SEQ}=1 \mid A(T+\Delta T)=1, B(T+\Delta T)=1,\\ C(T+\Delta T)=1\}=1. \end{cases} \tag{12}$$

3.2.3. Spare Gate. The spare gate includes a main part and several backup parts. After the main part fails, the first backup part starts to operate instead of the main part. After the first backup part fails, the second backup part starts, and so on. The output event does not occur until all parts have failed. According to the numerical of dormancy factor α, the spare gate can be divided into three types: cold spare gate ($\alpha = 0$), warm spare gate ($0 < \alpha < 1$), and hot spare gate ($\alpha = 1$). Warm gate is discussed in this paper, as shown in Figure 7; other types of spare gates can be studied as special cases.

$$\begin{cases} P\{A(T+\Delta T)=1 \mid A(T)=0\}=\int_T^{T+\Delta T} f_A(t)\mathrm{d}t,\\ P\{A(T+\Delta T)=1 \mid A(T)=1\}=1,\\ P\{S(T+\Delta T)=1 \mid A(T)=0, S(T)=0\}=\int_T^{T+\Delta T} f_{\alpha S}(t)\mathrm{d}t,\\ P\{S(T+\Delta T)=1 \mid A(T)=1, S(T)=0\}=\int_T^{T+\Delta T} f_S(t)\mathrm{d}t,\\ P\{S(T+\Delta T)=1 \mid S(T)=1\}=1,\\ P\{\mathrm{WSP}=1 \mid A(T+\Delta T)=1, S(T+\Delta T)=1\}=1, \end{cases} \tag{13}$$

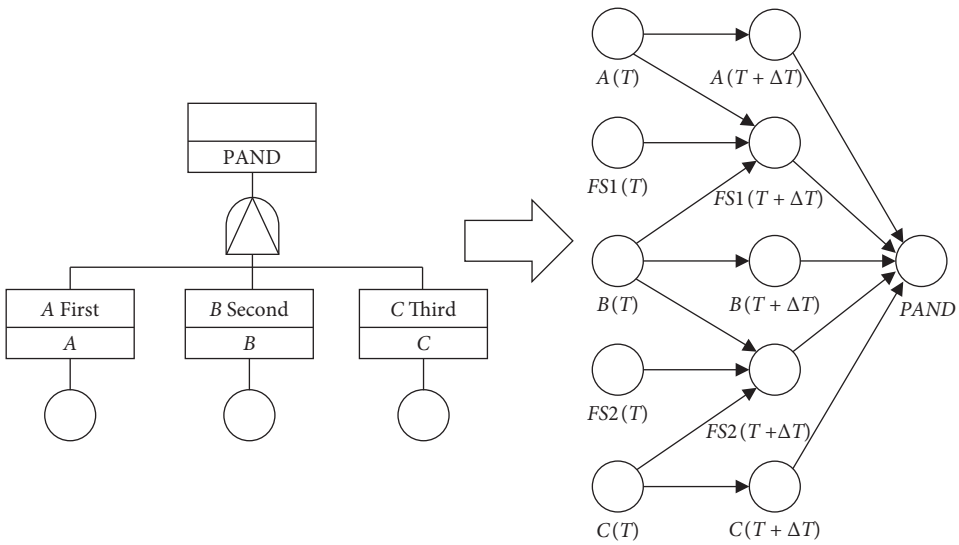

Figure 5: "Priority And gate" and the corresponding DBN model.

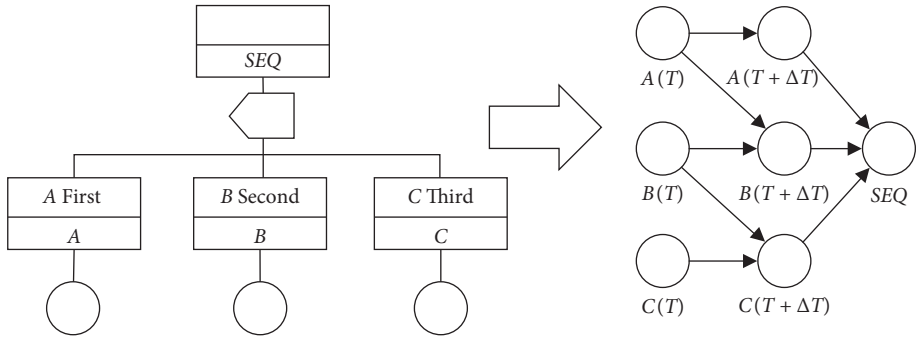

Figure 6: "Sequence-correlated gate" and the corresponding DBN model.

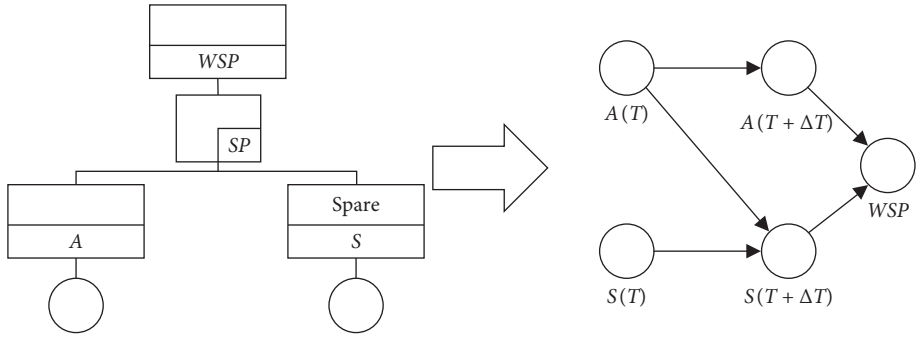

Figure 7: "Spare gate" and the corresponding DBN model.

where $f_{\alpha S}(t)$ is the failure density function of component S in the backup period.

3.2.4. Function-Correlated Gate. Function-correlated gate includes a trigger event and several related basic events, related basic events are repeatable event. According to the relationship between the trigger event and related basic events, Figure 8 shows the function-correlated gate which contains a trigger event and two related basic events, and the corresponding dynamic Bayesian network is shown as follows:

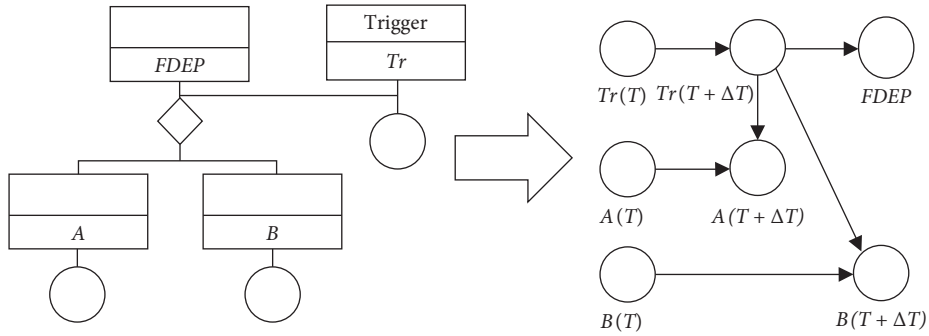

Figure 8: "Function-correlated" gate and the corresponding DBN model.

$$\begin{cases} P\{Tr(T+\Delta T)=1 \mid \mathrm{Tr}(T)=0\} = \int_{T}^{T+\Delta T} f_{\mathrm{Tr}}(t)\mathrm{d}t, \\ P\{Tr(T+\Delta T)=1 \mid \mathrm{Tr}(T)=1\} = 1, \\ P\{A(T+\Delta T)=1 \mid A(T)=0, \mathrm{Tr}(T+\Delta T)=0\} = \int_{T}^{T+\Delta T} f_{A}(t)\mathrm{d}t, \\ P\{A(T+\Delta T)=1 \mid \mathrm{Tr}(T+\Delta T)=1\} = 1, \\ P\{A(T+\Delta T)=1 \mid A(T)=1\} = 1, \\ P\{B(T+\Delta T)=1 \mid B(T)=0, \mathrm{Tr}(T+\Delta T)=0\} = \int_{T}^{T+\Delta T} f_{B}(t)\mathrm{d}t, \\ P\{B(T+\Delta T)=1 \mid Tr(T+\Delta T)=1\} = 1, \\ P\{B(T+\Delta T)=1 \mid B(T)=1\} = 1, \\ P\{\mathrm{FDEP}=1 \mid \mathrm{Tr}(T+\Delta T)=1\} = 1. \end{cases} \tag{14}$$

3.3. Fuzzy Possibility. When using DBN for evaluation, it is necessary to obtain the failure probability of the device, but in practical production, the integrity of data of each device cannot be guaranteed. In view of this, using fuzzy numbers and the defuzzification method to transform the experts' language into the failure rates is a practical solution. The fuzzy set theory was first proposed by zadeh and is often used to calculate the probability of fuzzy events. It is an effective way to deal with uncertainty or lack of information. In recent years, the combination of fuzzy set theory and Bayesian network has also been widely used in risk analysis and evaluation [32–36].

3.3.1. Expert Elicitation. Expert elicitation is essentially a scientific consensus methodology, often used for calculating the probabilities of vague events. This method is a solution for dealing with uncertainty and lack of sufficient data and provides useful information for assessing risks. Eight different conversion scales have been provided by [37]. In the present study, we use Scale 7 [VH, H, RH, M, RL, L, VL] (Table 1) for estimating the severity of an event. The reason for selecting scale number 7 is that humans' memory capacity is seven plus-minus two chunks, and the linguistic terms are in the form of trapezoidal fuzzy numbers [32].

3.3.2. Aggregation of Fuzzy Number. Since experts are different in knowledge and views, in order to reach a consensus among them, it is required to integrate the assigned terms by

Table 1: 7 conversion scales for estimating the likelihood of events.

Linguistic term	Description	Fuzzy set
Very high (VH)	Once in a month	(0.8, 0.9, 1, 1)
High (H)	Once in every 1 to 3 months	(0.7, 0.8, 0.8, 0.9)
Relatively high (RH)	Once in every 3 to 6 months	(0.5, 0.6, 0.7, 0.8)
Medium (M)	Once in every 6 to 12 months	(0.4, 0.5, 0.5, 0.6)
Relatively low (RL)	Once in every 1 to 5 years	(0.2, 0.3, 0.4, 0.5)
Low (L)	Once in every 5 to 10 years	(0.1, 0.2, 0.2, 0.3)
Very low (VL)	Never happened	(0, 0, 0.1, 0.2)

experts to a single one. For the objectivity of the data, this paper categorizes experts' weighting criteria according to their education level, professional position, and experience time, as shown in Table 2. And five expert decisions are considered, and then expert language is converted into data. Table 3 shows some information about experts. Integrate the weights and fuzzy numbers of experts by linear weighting method, and equations (15) and (16), respectively, give expert weights and linear weighted integration.

$$w_i = \frac{\mathrm{ET\ score}(i) + \mathrm{EL\ score}(i) + \mathrm{PP\ score}(i)}{\sum_{i=1}^{n}\mathrm{ET\ score}(i) + \sum_{i=1}^{n}\mathrm{EL\ score}(i) + \sum_{i=1}^{n}\mathrm{PP\ score}(i)}, \tag{15}$$

where w_i refers to the weighting factor of the i-th expert, n of all experts, ET score, EL score and PP score are shown in Table 2.

$$\widetilde{A}_j = \sum_{i=1}^{n} w_i \widetilde{A}_{ij}, \quad j = 1, 2, \ldots, m, \tag{16}$$

where $\widetilde{A}_j$ is an aggregate fuzzy number of basic events, $\widetilde{A}_{ij}$ is the fuzzy probability assigned by an expert, n of all experts, and m of all events.

3.3.3. Defuzzification. To draw useful results for decision making, the fuzzy probability of the basic and conditional events must be mapped to crisp number through defuzzification, and this facilitates computational reasoning in

Table 2: Weighting criteria of different experts.

Nature attribute	Classification	Score
Experience time (ET)	≥30 years	5
	20 to 29 years	4
	10 to 19 years	3
	6 to 9 years	2
	≤5 years	1
Education level (EL)	Doctorate	5
	Master's degree	4
	Bachelor's degree	3
	Junior college	2
	School leaver	1
Professional position (PP)	Chief engineer/Senior academic	5
	Manager	4
	Engineer/Junior academic	3
	Technician	2
	Operator	1

Table 3: Expert information.

Experts	Professional position (PP)	Experience time (ET)	Education level (EL)	Weight score (ω)
E1	Junior academic	3 years	Master's degree	0.216216216
E2	Operator	2 years	Bachelor's degree	0.135135135
E3	Engineer	12 years	Bachelor's degree	0.243243243
E4	Junior academic	3 years	Master's degree	0.216216216
E5	Junior academic	2 years	Bachelor's degree	0.189189189

DBN. A trapezoidal fuzzy function can be defined as in Figure 9, defuzzification of the trapezoidal fuzzy number $\widetilde{A} = (a_1, a_2, a_3, a_4)$ based on the center of area method can be calculated as equation (17).

$$\begin{aligned} \mathrm{COG}(\widetilde{A}) &= \frac{\int \mu_{\widetilde{A}}(x)x\,\mathrm{d}x}{\int \mu_{\widetilde{A}}(x)\mathrm{d}x} = \frac{\int_{a_1}^{a_2}((x-a_1)/(a_2-a_1))\cdot x\mathrm{d}x + \int_{a_2}^{a_3} x\,\mathrm{d}x + \int_{a_3}^{a_4}((a_4-x)/(a_4-a_3))\cdot x\,\mathrm{d}x}{\int_{a_1}^{a_2}((x-a_1)/(a_2-a_1))\mathrm{d}x + \int_{a_2}^{a_3}\mathrm{d}x + \int_{a_3}^{a_4}((a_4-x)/(a_4-a_3))\mathrm{d}x}, \\ &= \frac{1}{3}\cdot\frac{(a_4+a_3)^2 - a_3a_4 - (a_1+a_2)^2 + a_1a_2}{a_3+a_4-a_1-a_2}. \end{aligned} \tag{17}$$

The last step is to convert fuzzy possibility (FP) of vague events into fuzzy probability (FPr). A function developed by (18) is used for converting FPs to FPr:

$$\mathrm{FPr} = \begin{cases} 10^{-\left[2.301\times\left(\frac{1-\mathrm{FPs}}{\mathrm{FPs}}\right)^{(1/3)}\right]} & \text{if FPs} \neq 0, \\ 0 & \text{if FPs} = 0, \end{cases} \tag{18}$$

where FPs is fuzzy possibility and FPR is fuzzy probability for each event.

4. Case Studies

4.1. DBT Modeling. Through the analysis of the coal water slurry gasification process, combined with the HAZOP analysis report and expert opinions, the risk factors that lead to the overheating of the gasifier are identified, and the dynamic butterfly model shown in Figure 10 is constructed. Table 3 shows five experts' information, Table 4 describes the basic events in the model. The model shows the evolution process of risk factors to accidents and accidents to consequences through dynamic fault trees and event trees.

It can be seen from Figure 10 that high oxygen-coal ratio, poor atomization effect of the burner, and low coal slurry concentration are the three main factors that lead to gasifier overheating. The oxygen-coal ratio is a key index for regulating the operating temperature of gasification in the production process. The fluctuation of the oxygen-coal ratio is mainly due to the abnormal feeding, the interruption of the coal slurry supply, or the sudden increase of the oxygen feed, so that the oxygen-coal ratio is higher than the set value, and the temperature of the gasifier also increases immediately. The atomization effect of the burner is closely related to the performance of the burner. If the pressure difference of the burner is low, the atomization effect will be significantly reduced, and the central-oxygen ratio is

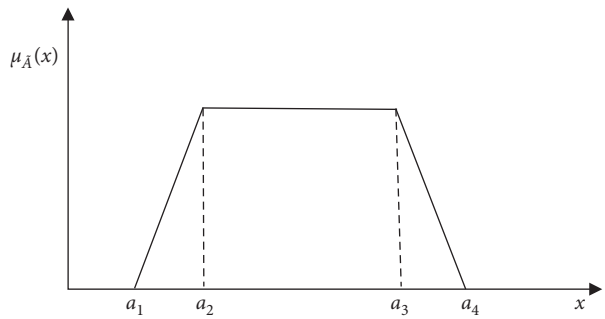

Figure 9: Trapezoidal fuzzy number $\tilde{A}$.

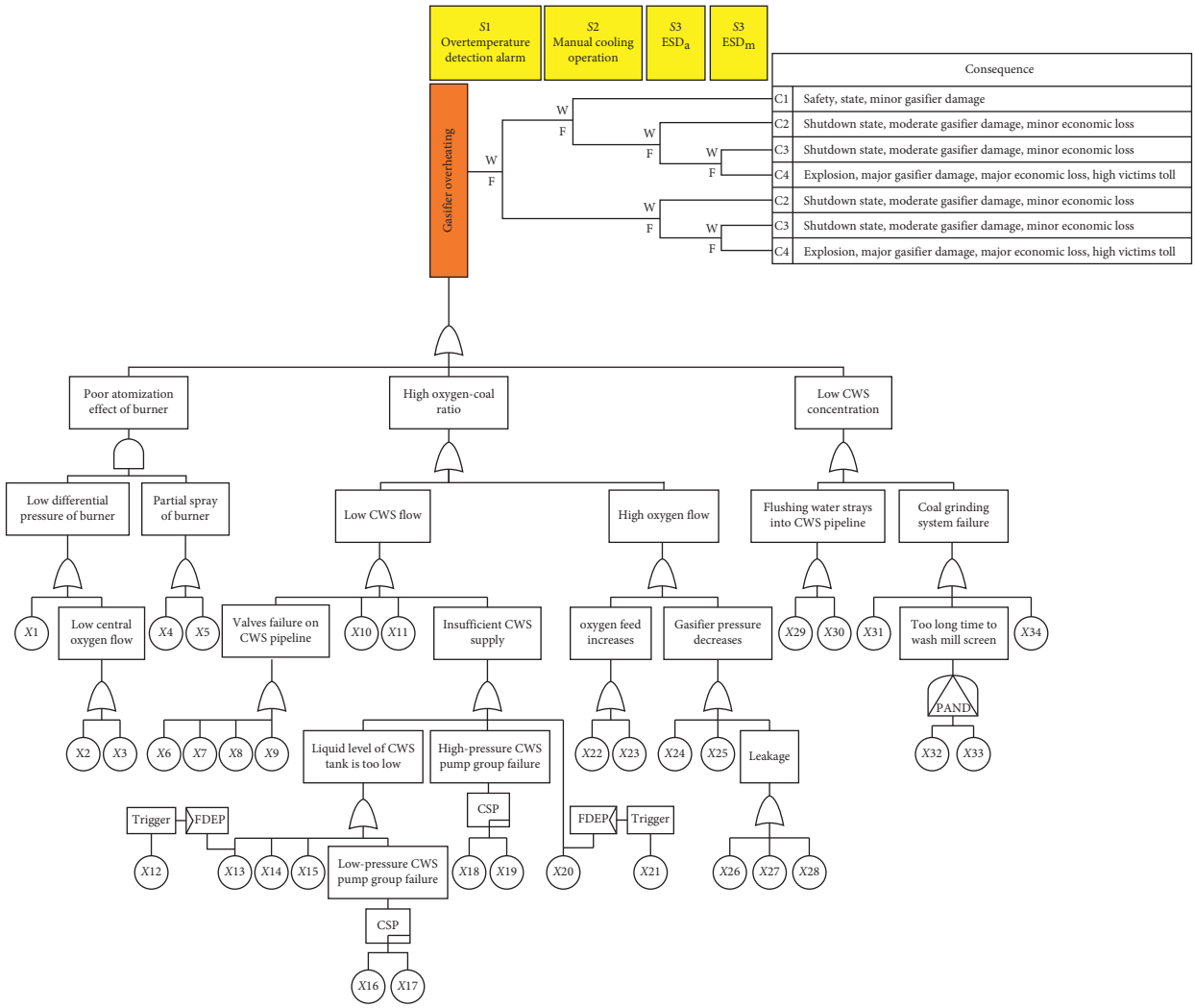

Figure 10: DBT model of gasifier overheating.

the main factor affecting the pressure difference of the burner. As the time elapsed, the burner is sprayed because uneven wear of coal slurry is also a factor that causes the atomization effect to deteriorate. The low concentration of coal slurry is mainly due to the failure of the pulping section or excessive flushing water entering the coal slurry line, which leads to a reduction in gasification efficiency and an increase in oxygen consumption, then leads to overheating of the gasifier. According to this model, it can be seen that a safety barrier is adopted in the project to prevent the expansion of the overheating accident of the gasifier, but the four safety barriers will also fail, resulting in different accident consequences. In this paper, the information of experts on basic events and safety barrier failure evaluation is transformed into corresponding fuzzy numbers according to equations (15)–(18).

Table 4: Basic event description and related data.

Symbol	Description	Failure model	Experts' judgement					Fps	Fpr (λ)	μ
			E1	E2	E3	E4	E5			
$X1$	Burner wear	Facilities failure	RH	RL	H	RH	H	0.674325	1.57E-02	0.25
$X2$	Center-oxygen flow valve failure	Facilities failure	RL	VL	M	M	M	0.410953	2.54E-03	0.125
$X3$	Blockage of center-oxygen check valve	Facilities failure	RL	VL	L	RL	RL	0.276973	6.79E-04	0.25
$X4$	Blockage of CWS pipeline at gasifier head	Facilities failure	M	VL	VL	RL	L	0.251819	4.92E-04	0.25
$X5$	Blockage of burner	Facilities failure	M	L	L	RL	L	0.297298	8.61E-04	0.25
$X6$	Drain valve of CWS pipeline opened by error	Operational error	L	L	L	M	L	0.264865	5.84E-04	—
$X7$	CWS circulating valve opened by error	Operational error	L	L	VL	M	VL	0.213133	2.78E-04	—
$X8$	Leakage of CWS circulating valve	Facilities failure	L	L	L	RH	L	0.297298	8.61E-04	0.125
$X9$	CWS block valve closed by error	Operational error	L	RL	VL	M	VL	0.233172	3.79E-04	—
$X10$	Blockage of CWS pipeline	Facilities failure	RH	L	VL	RL	RL	0.328724	1.20E-03	0.25
$X11$	Leakage of CWS pipeline	Facilities failure	RL	VL	VL	M	L	0.251819	4.92E-04	2
$X12$	Agitator failure in the mill discharge tank	Facilities failure	L	RL	VL	RL	L	0.223507	3.27E-04	0.25
$X13$	Blockage of low-pressure CWS pump inlet	Facilities failure	M	L	VL	M	RL	0.329061	1.21E-03	0.25
$X14$	Coal mill failure	Facilities failure	L	M	VL	RH	L	0.308765	9.77E-04	0.5
$X15$	Manhole leaks in the CWS tank	Facilities failure	RL	VL	VL	RL	L	0.219144	3.06E-04	0.5
$X16$	Low-pressure CWS primary pump failure	Facilities failure	RL	L	L	L	L	0.232433	3.75E-04	0.33
$X17$	Low-pressure CWS standby pump failure	Facilities failure	L	L	VL	VL	VL	0.121677	3.57E-05	0.33
$X18$	High-pressure CWS primary pump failure	Facilities failure	RL	VL	RL	RL	RL	0.313381	1.03E-03	0.33
$X19$	High-pressure CWS standby pump failure	Facilities failure	L	VL	VL	VL	VL	0.104881	1.98E-05	0.33
$X20$	Blockage of high-pressure CWS pump inlet	Facilities failure	M	L	L	M	RL	0.358108	1.60E-03	2
$X21$	Agitator failure in the CWS tank	Facilities failure	L	VL	L	RL	L	0.216358	2.93E-04	0.25
$X22$	The opening of oxygen flow valve is too large	Operational error	L	M	RL	RL	RL	0.33784	1.32E-03	—
$X23$	The pressure of oxygen buffer tank outlet is too high	Operational error	L	RL	VL	M	VL	0.233172	3.79E-04	—
$X24$	Safety valve of carbon washing tower opened by error	Operational error	L	L	VL	RL	L	0.203358	2.36E-04	—
$X25$	Syngas purge valve opened by error	Operational error	L	RL	VL	RL	VL	0.200452	2.24E-04	—
$X26$	Leakage of pipeline connected with gasifier	Facilities failure	M	M	VL	M	RL	0.369603	1.78E-03	0.33
$X27$	Leakage of flange connected with gasifier	Facilities failure	RL	RH	RL	RH	M	0.483786	4.45E-03	0.33
$X28$	Leakage of lock hopper	Facilities failure	M	RH	VL	M	L	0.361554	1.65E-03	0.33
$X29$	Leakage of slurry flush valve	Facilities failure	RL	VL	L	RH	L	0.313537	1.03E-03	0.125
$X30$	Slurry flush valve opened by error	Operational error	L	RL	L	M	L	0.285136	7.48E-04	—
$X31$	Blockage of coal bunker outlet	Facilities failure	RL	RL	VL	H	M	0.409993	2.52E-03	0.25
$X32$	Blockage of coal mill screen	Facilities failure	RH	RH	VL	H	RH	0.543641	6.75E-03	0.25
$X33$	Slurry flush valve failed to close	Operational error	L	L	VL	L	VL	0.148269	7.57E-05	—
$X34$	The opening of mill feed water flow valve is too large	Operational error	L	M	L	RL	L	0.272975	6.46E-04	—
$S1$	Overheating detection alarm failure	Multiple failure	M	RL	RL	RL	M	0.321622	1.12E-03	—
$S2$	Manual cooling operation failure	Multiple failure	M	RL	M	RH	RL	0.366216	1.73E-03	—
$S3$	ESD_a failure	Multiple failure	RL	RL	M	RL	RL	0.297298	8.61E-04	—
$S4$	ESD_m failure	Multiple failure	L	M	RL	RL	RL	0.20259	2.33E-04	—

The evaluation information of experts is converted into fuzzy numbers corresponding to basic events and safety barriers according to equations (15)–(18) in this paper. Then convert fuzzy numbers into fuzzy possibility (FP) based on center of gravity, and fuzzy probability for each event is calculated be equation [17]. In addition, due to the maintainability of the equipment, this paper also calculates the maintenance rate (μ) of the equipment. The above calculation data are shown in Table 4.

4.2. DBN Modeling. Figure 11 shows the DBN modeling for gasifier overheating and the simulation is based on application software (GeNie) which is an intuitive and easy-to-use software supporting a variety of inference algorithms. The DBN modeling of gasifier overheating is firstly established on the conversion algorithm including graphical and numerical conversion [25]. The graphical structure is obtained by the conversion of fault tree and event tree which are connected by the central node transformed from the central event. In fault tree, input and output of logic gate turn into parent node and child node linked by directed arcs. In event tree, all possible consequences integrate into one consequence node and all safety barriers turn into safety nodes. Both safety nodes and central node are linked with the consequence node. The node generally takes two states to indicate the occurrence and non-occurrence of the event. In this study, the nodes of the basic events, intermediate events, and central event are represented by "Y" and "N", the safety nodes are represented by "W" and "F", "Y" indicates that the event occurs, and "W" indicates that the safety barrier has successfully prevented escalation of the accident. Especially,

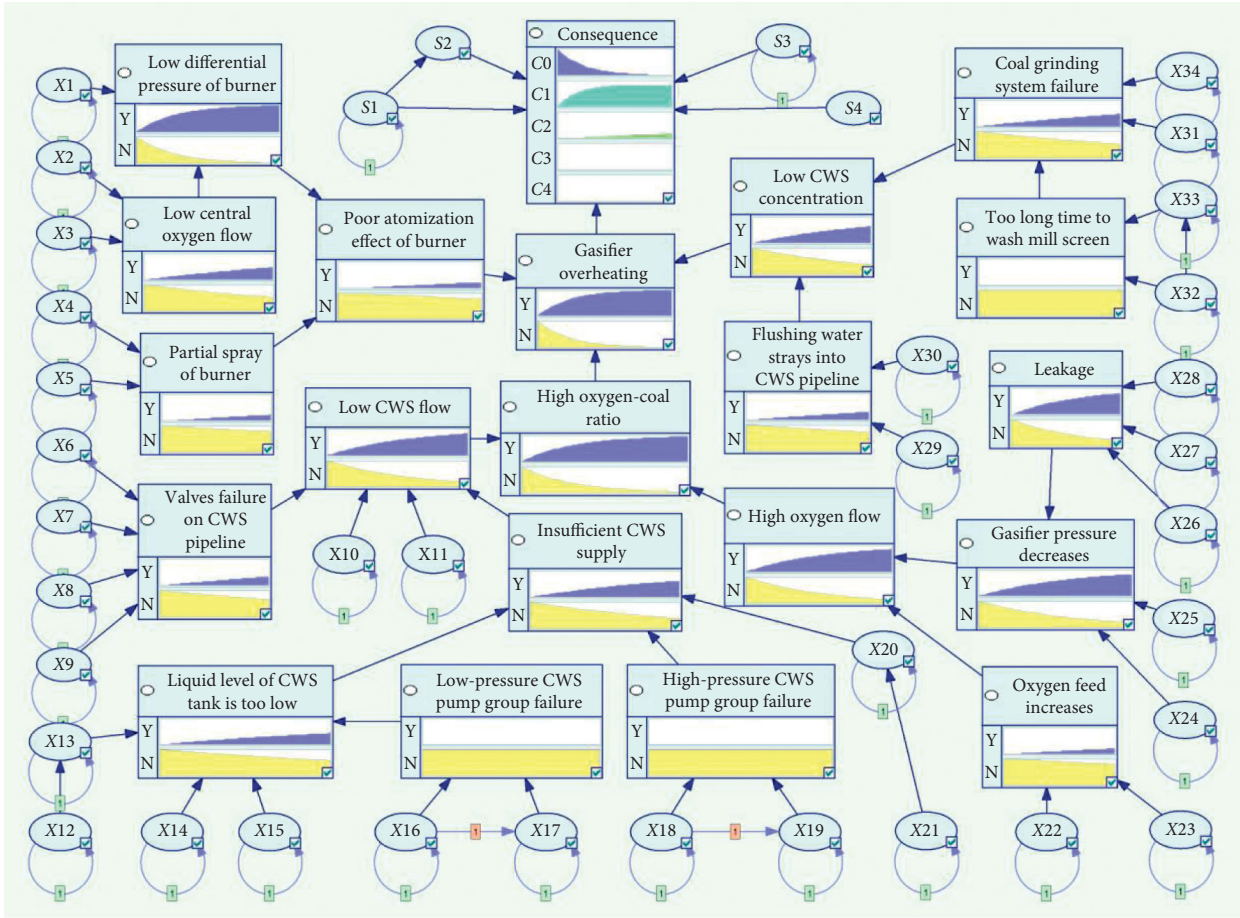

Figure 11: DBN model of gasifier overheating.

the consequence node consists of five states which contains\ identified possible consequences C1–C4, and the added "C0" state is set to indicate that the gasifier is not overheating.

The dynamic evolution of events has not been described through the above procedure because directed arcs only connect nodes in the same time slice. In order to accomplish the expansion of BN on the time slice, assume that the probability of fault occurrence follows exponential distribution. Therefore, the nodes of basic events are selected as dynamic nodes, and considering that safety barriers $S1$ and $S3$ are controlled by electronic systems, safety nodes $S1$ and S3 are dynamic nodes too. As shown in Figure 3, the dynamic node has a directed arc from itself in addition to linking with other nodes; that is, the node under the previous time slice is the parent node of it under the present time slice. Moreover, dynamic logic gates are added in BT modeling to represent the dynamic dependencies between events, and the connection between nodes is based on the mapping rule of logical gate to DBN in the section 2.

Prior probability and CPT need to be determined for quantitative analysis in DBN. FPr calculated by expert evaluation serves as prior probability, the result is shown in Table 3. A node's CPT can be calculated by the mapping rules of logic gates in section 3, which consists of conditional probabilities under all its parent nodes. The conditional probability is calculated by probability density function for nodes between different time slices, and relevant calculation parameters μ, λ are also listed in Table 3. For safety barriers, the failure of overheating alarm leads to the failure of manual cooling operation; conditional probability is expressed as $P(S2 = F|S1 = F) = 1$ and other safety barriers are independent of each other. Developing 52 time slices after prior probability and conditional probability are input into GeNie, every time slice represents 1 week.

4.3. Dynamic Risk Analysis

4.3.1. Predictive Analysis. The probability of gasifier overheating can be predicted based on DBN forward reasoning, causality, and prior probability of events. Figure 12 shows the probability of an over-temperature accident in the gasifier operating 52 weeks (1 year) with and without maintenance. It can be seen from the Figure 12 that in the first four weeks of gasifier operation, the probability of overheating accidents is not greatly affected by maintainability. What is especially worth noticing is that the probability of overheating of the gasifier will increase monotonically with time, so if no maintenance measures are taken within 52 weeks, the probability of accidents will be as high as 0.983. However, maintenance can be used to reduce

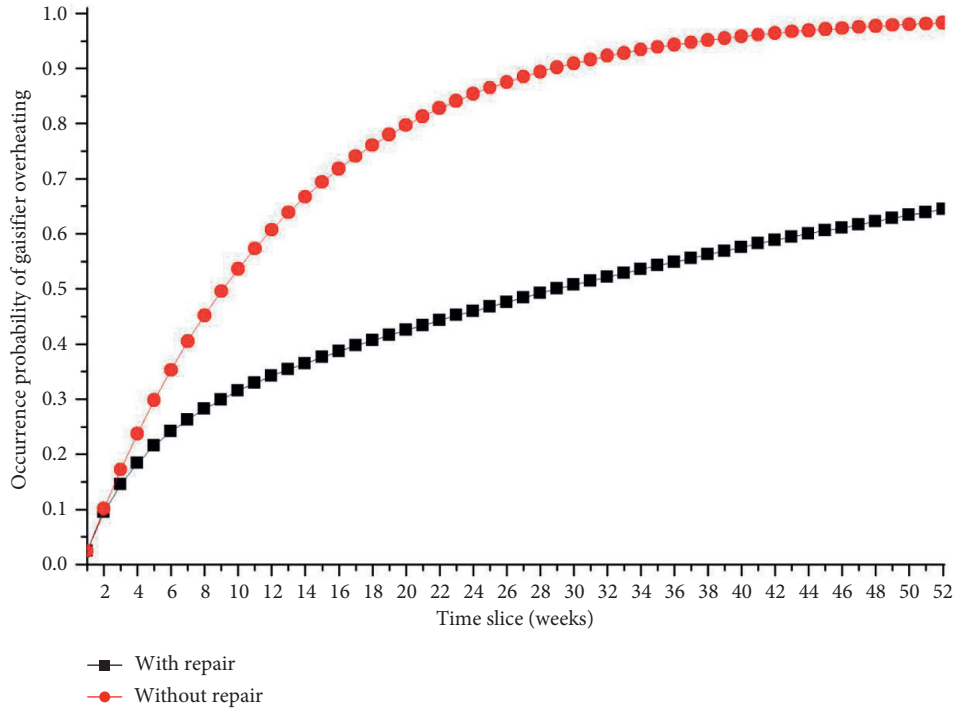

Figure 12: Dynamic probability prediction of gasifier overheating.

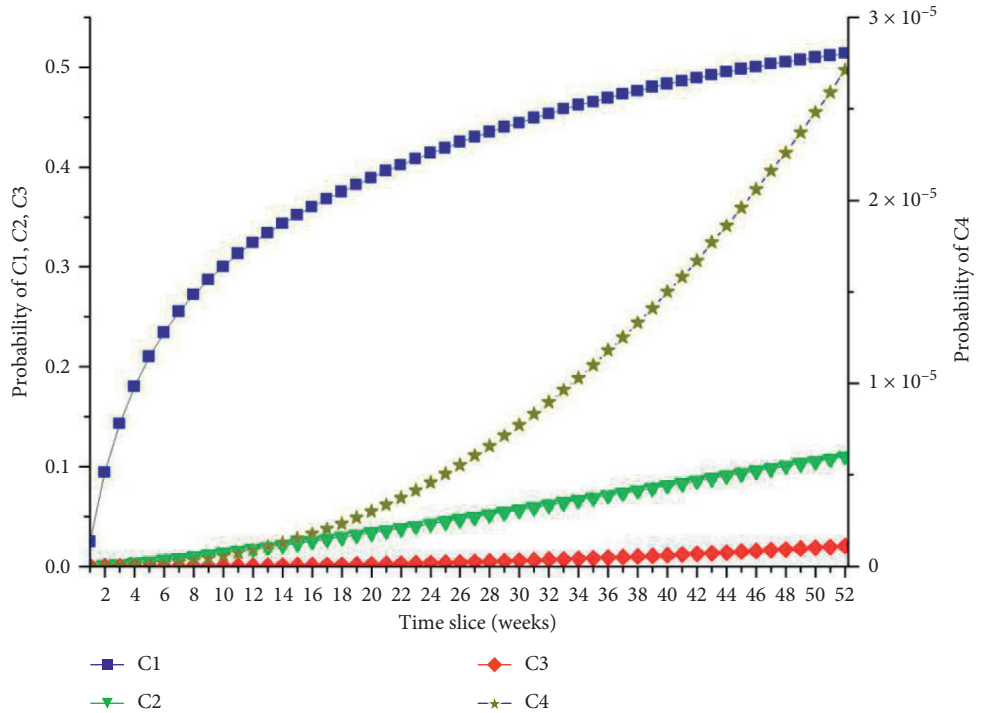

Figure 13: Dynamic probability prediction of consequence C1–C4.

the probability of accidents during operation, which shows the importance of maintenance measures for safe operation of the device.

Through DBN's forward reasoning, the probability of overheating causing different consequences can also be predicted. As shown in Figure 13, the probability of occurrence of each consequence also increases with time, the probability of the consequences $C1$, $C2$, $C3$, and $C4$ under the action of four safety barriers in Week 52 are 5.14E-01, 1.10E-01, 2.05E-02, 2.71E-05. Therefore, under the protection of the safety barrier, there is still a 51.4% probability that it can work normally even if the gasifier is over-temperature,

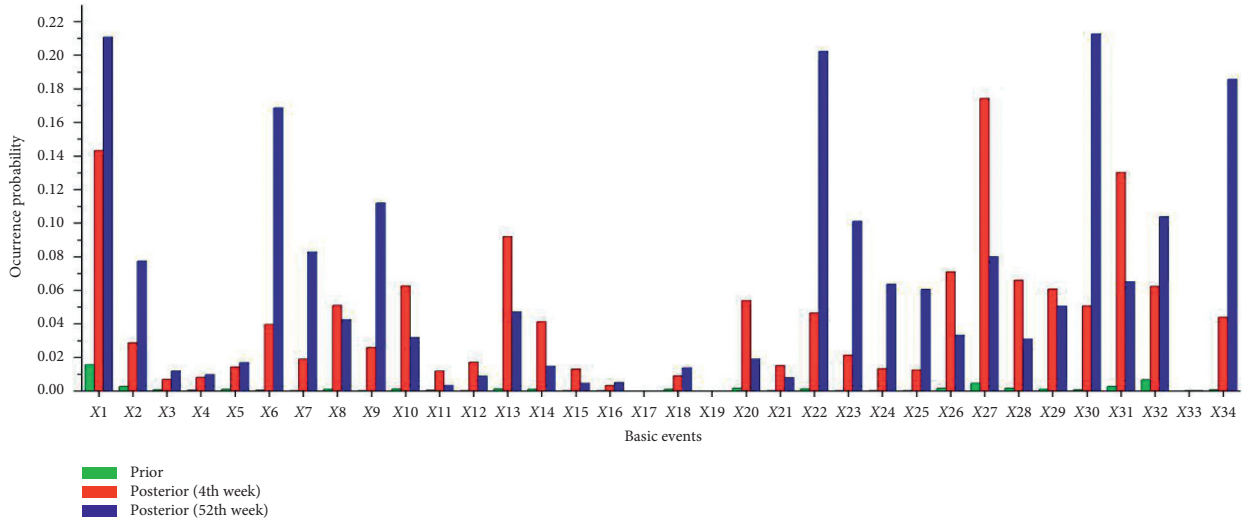

Figure 14: Comparison of prior probability and posterior probability of basic events.

thereby effectively avoiding further expansion of the accident. *C*2 and *C*3 are much larger than C4, indicating that even if the cooling the temperature fails, the emergency shutdown can still effectively prevent the accident from worsening. This also illustrates the importance of maintaining the normal operation of the emergency parking system.

4.3.2. Diagnostic Reasoning. It can be seen from above that the probability of overheating accidents in gasifiers is very high. Although the danger level can be reduced through maintenance and safety barriers, there are hidden dangers of untimely maintenance or failure of safety barriers. Thus, it is necessary to identify the key events that affect gasifier overheating and locate its weak links. DBN's diagnostic reasoning is a process from the child node to the parent node, dedicated to identifying the weak links in the whole risk scenario. This paper sets the gasifier overheating to "Yes", then the posterior probability of the basic event at any time segment can be obtained, Figure 14 shows the posterior probabilities of weeks 4 and 52 for all basic events. In previous studies, the production process has not been divided into time segments for safety evaluation.

Figure 14 compares the prior probability, the posterior probabilities of weeks 4 and 52, the results show that the basic events with higher posterior probability in week 4 are *X*27, *X*1, *X*31, *X*13, and *X*26, and the basic events with higher posterior probability in week 52 are *X*30, *X*1, *X*22, *X*34, and *X*6. The comparison results show that the main event leading to gasifier overheating is equipment failure when running for about one month, while after a year, operation error is the main factor leading to gasifier overheating. Comparison results show attention should be paid to equipment maintenance at the initial stage, while one year later, safety management needs more attention to avoid accidents caused by operational errors.

5. Conclusions

(1) Based on fuzzy mathematics and DBN, a quantitative dynamic risk analysis of gasifier overheating was carried out. For the problem of incomplete historical data of equipment in the actual production process, fuzzy logic concepts were employed, which convert the experts' linguistic judgement to aggregated results in the aggregation process, and this method was feasible.

(2) The DBN model of gasifier overheating was constructed, dynamic change law of equipment failure rate when system running for 1 year was obtained by forward reasoning method. According to DBT converted to DBN, the main event leading to gasifier overheating is equipment failure when running for about one month, while after a year, operation error is the main factor leading to gasifier overheating. At the same time, the maintenance factor was also considered, and the impact on the system failure risk analysis when repaired or not is compared.

(3) Based on the reasoning function of DBN, fault diagnosis of gasifier overheating was carried out. The prior probability of root nodes was obtained by fuzzy set theory, and then posterior probability of root nodes were deduced and sorted by the powerful reverse inference function of DBN; thus, the weakness of the system were identified. The calculation results show that with the prolonging of time and the increase of "precursor incident", equipment failure probability and accident risk show a significant growth trend.

Data Availability

The data of numerical results were generated during the study.

Conflicts of Interest

The authors declare that they have no conflicts of interest.

Acknowledgments

The authors are grateful for National project funding for Key R & D programs under Grant no. 2018YFC0808500, Scientific Research Project of the Department of Education of Liaoning Province (No. L2019044), and the Natural Science Foundation of Liaoning Province (No. 2019-ZD-0056).

References

[1] Y. Gong, Q. Zhang, H. Zhu, Q. Guo, and G. Yu, "Refractory failure in entrained-flow gasifier: Vision-based macrostructure investigation in a bench-scale OMB gasifier," *Applied Energy*, vol. 205, pp. 1091–1099, 2017.

[2] M. Gräbner and B. Meyer, "Performance and exergy analysis of the current developments in coal gasification technology," *Fuel*, vol. 116, pp. 910–920, 2014.

[3] D. Heguy and V. Rai, "Technology development and learning: coal gasification in China and the United States," *The Electricity Journal*, vol. 27, no. 6, pp. 69–85, 2014.

[4] X. Feng, Q. Zhang, E. Wang, M. Ali, Z. Dong, and G. Zhang, "3D modeling of the influence of a splay fault on controlling the propagation of nonlinear stress waves induced by blast loading," *Soil Dynamics and Earthquake Engineering*, vol. 138, Article ID 106335, 11 pages, 2020.

[5] X. Feng, Q. Zhang, and M. Ali, "Explosion-induced stress wave propagation in interacting fault system: Numerical modeling and implications for Chaoyang coal mine," *Shock and Vibration*, vol. 2019, Article ID 5856080, 12 pages, 2019.

[6] X. Feng and Q. Zhang, "The effect of backfilling materials on the deformation of coal and rock strata containing multiple goaf: A numerical study," *Minerals*, vol. 8, no. 6, p. 224, 2018.

[7] A. K. Goodwin and G. L. Rorrer, "Modeling of supercritical water gasification of xylose to hydrogen-rich gas in a hastelloy microchannel reactor," *Industrial & Engineering Chemistry Research*, vol. 50, no. 12, pp. 7172–7182, 2011.

[8] C. Y. Wen and T. Z. Chaung, "Entrainment coal gasification modeling," *Industrial & Engineering Chemistry Process Design and Development*, vol. 18, no. 4, pp. 684–695, 1979.

[9] E. J. Cialkowski and Y. Q. Li, "Assessment of neighbor-initiated risks in an integrated air separation unit-gasification facility," *Process Safety Progress*, vol. 38, no. 3, pp. 1–5, 2019.

[10] A. N. Rollinson, "Fire, explosion and chemical toxicity hazards of gasification energy from waste," *Journal of Loss Prevention in the Process Industries*, vol. 54, pp. 273–280, 2018.

[11] Y. Yun, J. H. Gu, and S. W. Chung, "Accident cases and safety issues in gasification plants," in *Proceedings of the 6th International Conference on Solid Waste Management 2016*, pp. 695–705, Springer, Kolkata, India, 2019.

[12] F. Sun, W. Xu, G. Wang, and B. Sun, "A technique to control major hazards of the coal gasification process developed from critical events and safety barriers," *Process of the Safety Progress*, vol. 36, no. 4, pp. 382–391, 2017.

[13] X. Xu, B. K. Zhang, X. Ma, and C. G. Wu, "Improvement & application of HAZOP analysis for batch process with SDG," in *Proceedings of the 2010 International Symposium on Intelligence Information Processing and Trusted Computing*, pp. 390–394, IEEE Computer Society, Huanggang, China, 2010.

[14] F.-J. Zuo, L. Yu, J. Mi, Z. Liu, and H.-Z. Huang, "Reliability analysis of gear transmission with considering failure correlation," *Ekspolatacja I Niezawodnosc - Maintenance and Reliability*, vol. 17, no. 4, pp. 617–623, 2015.

[15] Y. Chang, X. Wu, C. Zhang et al., "Dynamic Bayesian networks based approach for risk analysis of subsea wellhead fatigue failure during service life," *Reliability Engineering & System Safety*, vol. 188, pp. 454–462, 2019.

[16] S. N. Wu, L. B. Zhang, J. C. Fan, and Y. F. Zhou, "Dynamic risk analysis of hydrogen sulfide leakage for offshore natural gas wells in MPD phases," *Process Safety and Environmental Protection*, vol. 122, pp. 1–28, 2019.

[17] A. Meel and W. D. Seider, "Plant-specific dynamic failure assessment using Bayesian theory," *Chemical Engineering Science*, vol. 61, no. 21, pp. 7036–7056, 2006.

[18] M. Kalantarnia, F. Khan, and K. Hawboldt, "Modelling of BP Texas city refinery accident using dynamic risk assessment approach," *Process Safety and Environmental Protection*, vol. 88, no. 3, pp. 191–199, 2010.

[19] H. Pasman and G. Reniers, "Past, present and future of quantitative risk assessment (QRA) and the incentive it obtained from land-use planning (LUP)," *Journal of Loss Prevention in the Process Industries*, vol. 28, no. 11, pp. 2–9, 2014.

[20] C. Yeo, J. Bhandari, R. Abbassi, V. Garaniya, S. Chai, and B. Shomali, "Dynamic risk analysis of offloading process in floating liquefied natural gas (FLNG) platform using bayesian network," *Journal of Loss Prevention in the Process Industries*, vol. 41, pp. 259–269, 2016.

[21] E. Zarei, A. Azadeh, N. Khakzad, M. M. Aliabadi, and I. Mohammadfam, "Dynamic safety assessment of natural gas stations using bayesian network," *Journal of Hazardous Materials*, vol. 321, pp. 830–840, 2017.

[22] P. A. P. Ramírez and I. B. Utne, "Use of dynamic Bayesian networks for life extension assessment of ageing systems," *Reliability Engineering & System Safety*, vol. 133, pp. 119–136, 2015.

[23] S. Rebello, H. Y. Yu, and L. Ma, "An integrated approach for system functional reliability assessment using dynamic bayesian network and hidden markov model," *Reliability Engineering & System Safety*, vol. 180, pp. 124–135, 2018.

[24] N. Khakzad, G. Landucci, and G. Reniers, "Application of dynamic Bayesian network to performance assessment of fire protection systems during domino effects," *Reliability Engineering & System Safety*, vol. 167, pp. 232–247, 2017.

[25] N. Khakzad, F. Khan, and P. Amyotte, "Dynamic safety analysis of process systems by mapping bow-tie into Bayesian network," *Process Safety and Environmental Protection*, vol. 91, no. 1-2, pp. 46–53, 2013.

[26] Z. Bilal, K. Mohammed, and H. Brahim, "Bayesian network and bow tie to analyze the risk of fire and explosion of pipelines," *Process Safety Progress*, vol. 36, no. 2, pp. 202–212, 2017.

[27] Y. Chang, C. Zhang, J. Shi, J. Li, S. Zhang, and G. Chen, "Dynamic Bayesian network based approach for risk analysis of hydrogen generation unit leakage," *International Journal of Hydrogen Energy*, vol. 44, no. 48, pp. 26665–26678, 2019.

[28] S. Wu, L. Zhang, W. Zheng, Y. Liu, and M. A. Lundteigen, "A DBN-based risk assessment model for prediction and diagnosis of offshore drilling incidents," *Journal of Natural Gas Science and Engineering*, vol. 34, pp. 139–158, 2016.

[29] C. Zhang, H. Y. Wang, and Y. X. Wei, "Fuzzy reliability based bow tie analysis of coal mine water inrush risks," in *Proceedings of the 8th International Conference on Sustainable Development in the Minerals Industry*, vol. 2, pp. 89–94, Fort Myers, FL, USA, July 2017.

[30] J. Chen, P.-A. Zhong, R. An, F. Zhu, and B. Xu, "Risk analysis for real-time flood control operation of a multi-reservoir system using a dynamic Bayesian network," *Environmental Modelling & Software*, vol. 111, pp. 409–420, 2019.

[31] B. Cai, H. Liu, and M. Xie, "A real-time fault diagnosis methodology of complex systems using object-oriented Bayesian networks," *Mechanical Systems and Signal Processing*, vol. 80, pp. 31–44, 2016.

[32] E. Zarei, N. Khakzad, V. Cozzani, and G. Reniers, "Safety analysis of process systems using fuzzy bayesian network (FBN)," *Journal of Loss Prevention in the Process Industries*, vol. 57, pp. 7–16, 2019.

[33] R. He, X. Li, G. Chen, Y. Wang, S. Jiang, and C. Zhi, "A quantitative risk analysis model considering uncertain information," *Process Safety and Environmental Protection*, vol. 118, pp. 361–370, 2018.

[34] Y. Li, D. Xu, and J. Shuai, "Real-time risk analysis of road tanker containing flammable liquid based on fuzzy bayesian network," *Process Safety and Environmental Protection*, vol. 134, pp. 36–46, 2020.

[35] M. M. Aliabadi, A. Pourhasan, and I. Mohammadfam, "Risk modelling of a hydrogen gasholder using fuzzy bayesian network (FBN)," *International Journal of Hydrogen Energy*, vol. 45, no. 1, pp. 1177–1186, 2020.

[36] M. Li, D. Wang, and H. Shan, "Risk assessment of mine ignition sources using fuzzy bayesian network," *Process Safety and Environmental Protection*, vol. 125, pp. 297–306, 2019.

[37] S. J. J. Chen, C. L. Hwang, M. J. Beckmann, and W. Krelle, *Fuzzy Multiple Attribute Decision Making Methods*, Springer, Berlin, Germany, 1992.